

## Article

# Lanthanide(III) Complexes with Thiodiacetato Ligand: Chemical Speciation, Synthesis, Crystal Structure, and Solid-State Luminescence

Julia Torres <sup>1</sup>, Javier González-Platas <sup>2</sup> and Carlos Kremer <sup>1,\*</sup>

<sup>1</sup> Área Química Inorgánica, Departamento Estrella Campos, Facultad de Química, Universidad de la República, Montevideo 11800, Uruguay

<sup>2</sup> Departamento de Física, Instituto Universitario de Estudios Avanzados en Física Atómica, Molecular y Fotónica (IUDEA), MALTA-Cosolider Team, Universidad de La Laguna, E-38206 La Laguna, Tenerife, Spain

\* Correspondence: ckremer@fq.edu.uy

**Abstract:** The synthesis, crystal structures, and luminescence of two lanthanide polynuclear complexes with the general formula  $[\text{Ln}_2(\text{tda})_3(\text{H}_2\text{O})_5] \cdot 3\text{H}_2\text{O}$  ( $\text{Ln} = \text{Sm}, \text{Eu}$ ; tda = thiodiacetato anion) are reported. The compounds were obtained by direct reaction of  $\text{H}_2\text{tda}$  and lanthanide(III) chloride in an aqueous solution. The choice of the conditions of synthesis was based on speciation studies. The structure of the polymeric complexes contains Ln(III) ions in a tricapped trigonal prism geometry. The versatility of this ligand provides different coordination modes and provokes the formation of thick 2D sheets. Direct excitation of the Ln(III) ions gives place to the characteristic intra-configuration sharp luminescence emission of both complexes in the solid state.

**Keywords:** lanthanide complexes; crystal structure; chemical speciation; thiodiacetato complex



**Citation:** Torres, J.; González-Platas, J.; Kremer, C. Lanthanide(III) Complexes with Thiodiacetato Ligand: Chemical Speciation, Synthesis, Crystal Structure, and Solid-State Luminescence. *Crystals* **2023**, *13*, 56. <https://doi.org/10.3390/cryst13010056>

Academic Editor: László Kovács

Received: 8 December 2022

Revised: 21 December 2022

Accepted: 24 December 2022

Published: 28 December 2022



**Copyright:** © 2022 by the authors. Licensee MDPI, Basel, Switzerland. This article is an open access article distributed under the terms and conditions of the Creative Commons Attribution (CC BY) license (<https://creativecommons.org/licenses/by/4.0/>).

## 1. Introduction

The study of lanthanide(III) (Ln) coordination compounds has elicited considerable interest in the last decades [1–4]. Different coordination numbers and geometries can give place to novel and interesting crystal structures. In addition, they have great potential as functional solid materials such as luminescent materials [5], magnetic devices [6], chemical sensors [7,8], etc. We and other groups have been interested in Ln(III) mononuclear and polynuclear complexes with ligands of type  $\text{X}-(\text{CH}_2-\text{COO})_2^{2-}$ , where  $\text{X} = \text{O}$  (oxydiacetato, oda<sup>2-</sup>),  $\text{NH}$  (iminodiacetato, ida<sup>2-</sup>) or  $\text{S}$  (thiodiacetato, tda<sup>2-</sup>) [9]. Oxydiacetato, the most deeply studied ligand of this group, appears as the most suitable ligand for Ln ions because of the presence of three O donor atoms in its structure. Hence, many complexes were already reported and characterized [9–13]. The thermodynamic stability of Ln-oda complexes also allows the use of the tris-chelate ( $[\text{Ln}(\text{oda})_3]^{3-}$ ) as a complex-as-ligand block towards M(II) cations [9,14]. The resulting heteropolynuclear compounds were assayed as catalysts [15,16], white-light emitters [17], and proton conductive MOF-based materials [18]. Iminodiacetato, with an N atom in the center, has also been studied, but to a lesser extent [9]. Substitution of O in oda by N in ida provokes a poorer participation of N in the coordination [14,19], which has hindered the isolation of tris-chelates.

Thiodiacetato is the less explored member of this series of ligands. The combination of O-carboxylate (hard donor atom) with sulfur (soft donor atom) makes the chemistry of this ligand very versatile and, at the same time, very challenging. Several structural reports show its capacity to act as a tridentate ligand towards Cu(II) [20–23], Ni(II) [24–29] Co(II) [30–36], Mn(II) [37], Zn(II) [38–40], Cd(II) [41], Mg(II) [42], Re(V) [43], V(IV) [44], and Ru(III) [45]. However, only one report can be found containing a bis-chelated fragment in a mononuclear compound [32], namely,  $(\text{pipH}_2)[\text{Co}(\text{tda})_2] \cdot 2\text{H}_2\text{O}$  ( $\text{pipH}_2^{2+} = \text{piperazine dication}$ ). The other structures always contain a coligand. The possibility of acting as

a bidentate ligand (O,O or O,S) for these metal ions is restricted to a few cases [46,47]. Thiodiacetato ligand also exhibits the possibility of forming a bridge between metal ions, yielding polynuclear complexes. This can be found in structures with Cu(II) [20,48–50], Mn(II) [37,49,51], and Zn(II) [52–54].

Coordination compounds of tda with Ln ions are even less frequent. Anionic isolated tris-chelates have been reported in  $(\text{H}_2\text{Gun})_3[\text{Ln}(\text{tda})_3]$  (Ln = Pr, Nd, HGun = guanidinium,  $\text{C}(\text{NH}_2)_3^+$ ) [55]. In these structures, tda acts as bidentate through two O-carboxylate atoms, forming an 8-membered ring. S atom is 3.423 Å apart from Ln ion and does not participate in the coordination sphere. Another report presents a polynuclear compound with the formula  $[\text{Nd}(\text{tda})(\text{H}_2\text{O})_4]\text{Cl}$  [56]. In this compound, tda acts as tridentate and additionally bridges Nd ions through carboxylate groups. A zigzag chain is formed. Nd(III) also forms an anionic 2D network in the complex  $\text{Na}[\text{Nd}(\text{tda})_2]$ , in which the S atom is not coordinated, and the coordination sphere is filled only by O atoms from tda [57]. The structure of  $(\text{pipH}_2)[\text{Ce}_2(\text{tda})_4(\text{H}_2\text{O})_2] \cdot 3\text{H}_2\text{O}$  is also a 2D anionic structure [58]. Finally, other groups of 2D polynuclear structures can be found. In  $[\text{Ln}_2(\text{tda})_3(\text{H}_2\text{O})_2]_n$  (Ln = La, Sm, Gd, Nd, Pr, Tb, Dy, Eu), tda acts as bidentate and also as a ditopic ligand. The S atom seems to participate in the coordination but at a rather long distance [59–63].

In order to increase the knowledge of tda as a ligand towards Ln ions, we have revisited the solution chemistry of the systems by potentiometry and prepared, under mild reaction conditions, complexes with the general formula  $[\text{Ln}_2(\text{tda})_3(\text{H}_2\text{O})_5] \cdot 3\text{H}_2\text{O}$  (Ln = Sm (1), Eu (2)). They show a new 2D structural arrangement. Solid-state luminescent properties were also studied.

## 2. Materials and Methods

All chemicals were reagent grade, purchased from commercial sources, and used without purification.  $\text{LnCl}_3 \cdot 6\text{H}_2\text{O}$  (Ln = Sm, Eu, 99.9% from Sigma-Aldrich, Burlington, MA, USA) were used as metal sources. Potentiometric measurements were carried out using an automatic titrator Mettler-Toledo DL50-Graphix. Elemental analyses (C, H, and S) were performed on a Thermo FLASH 2000 CHNS/O Analyzer instrument. Infrared spectra were collected as KBr pellets on an FTIR Shimadzu IR-Prestige-21 spectrophotometer from 4000 to  $400\text{ cm}^{-1}$ . Thermogravimetric analyses (TGA) were carried out on a Shimadzu TGA-50 instrument with a TA 50I interface, using a platinum cell and nitrogen atmosphere; the experimental conditions were  $0.5\text{ }^\circ\text{C min}^{-1}$  temperature ramp rate and  $50\text{ mL min}^{-1}$  nitrogen flow rate (pure nitrogen was used, water content was less than 3 ppm). Luminescence spectra were recorded from solid crystalline samples using a SHIMADZU RF-5301Pc spectrofluorometer.

### 2.1. Equilibrium Studies

The standard HCl and NaOH solutions were prepared by diluting Merck standard ampoules. Acid and base stock solutions were standardized against sodium carbonate and potassium hydrogen phthalate, respectively. All solutions were prepared with analytical-grade water ( $18\text{ }\mu\text{S cm}^{-1}$ ) and were freed of carbon dioxide by bubbling with argon.  $\text{NaClO}_4 \cdot \text{H}_2\text{O}$  (Sigma-Aldrich 98%) was used to adjust the ionic strength of all solutions to  $0.15\text{ mol}\cdot\text{L}^{-1}$ . The temperature was kept at  $25.0 (\pm 0.1)\text{ }^\circ\text{C}$ . The protonation constants of  $\text{tda}^{2-}$  were determined by two potentiometric titrations (*ca.* 150 experimental points each) in the interval  $1\text{--}8\text{ mmol}\cdot\text{L}^{-1}$ . The behavior of the ligand in the presence of either Sm(III) or Eu(III) was then analyzed through three potentiometric titrations (*ca.* 100–150 experimental points each) at ligand to Ln(III) total molar ratios varying from 1:1 to 3:1. The pH interval from 2.0 to the precipitation of solid  $\text{Ln}(\text{OH})_3$  in the alkaline region was covered.

In a typical experiment, after thermal equilibrium was reached, hydrogen ion concentrations were determined by successive readings, each performed after an incremental addition of standard  $0.1\text{ mol}\cdot\text{L}^{-1}$  NaOH solution. Equilibrium attainment after each titrant addition was verified by controlling the deviation of successive e.m.f. readings. Independent stock solutions were used to check reproducibility. The cell electrode potential  $E^\circ$

and the acidic junction potential were determined [64] from independent titrations of the strong acid with the titrant solution. The calibration in the alkaline range was checked by recalculating  $K_w$  values for each system. The obtained values (average  $\log_{10} K_w = 13.7$ ) were checked to be in line with previously reported data under the same experimental conditions [65]. The formation constant of soluble hydroxo species of Ln(III) was taken from a previous report [66] and was included in the input for the calculation of the formation constants. Further details on data analysis can be found elsewhere [67].

## 2.2. X-ray Data Collection and Structure Refinement

X-ray diffraction data on single crystals 1 and 2 were collected with an Agilent SuperNOVA diffractometer with microfocus X-ray using Mo  $K\alpha$  radiation ( $\lambda = 0.71073 \text{ \AA}$ ). CrysAlisPro [68] software was used to collect, index, scale and apply a numerical absorption correction based on Gaussian integration over a multifaceted crystal model. The structures were solved using ShelXT [69] program using dual methods and refined by full-matrix least-squares minimization on  $F^2$  using ShelXL [70] software. All non-hydrogen atoms were refined anisotropically. Hydrogen atom positions were calculated geometrically and refined using the riding model. The geometrical analysis of the interactions in the structures was performed with PLATON [71] and Olex2 [72] programs. Crystal data, collection procedures, and refinement results are summarized in Table 1.

**Table 1.** Crystallographic data and structure refinements for compounds 1 and 2.

Compound	1	2
Formula	$C_{12}H_{28}O_{20}S_3Sm_2$	$C_{12}H_{28}O_{20}S_3Eu_2$
$D_{calc}/g\text{ cm}^{-3}$	2.231	2.250
$\mu/\text{mm}^{-1}$	4.715	5.042
Formula Weight	889.22	892.44
Colour	colorless	colorless
Shape	block-shaped	irregular-shaped
Size/ $\text{mm}^3$	$0.17 \times 0.09 \times 0.07$	$0.07 \times 0.06 \times 0.04$
T/K	293(2)	293(2)
Crystal System	triclinic	triclinic
Space Group	$P-1$	$P-1$
$a/\text{\AA}$	9.0767(3)	9.0706(3)
$b/\text{\AA}$	12.1931(4)	12.1653(3)
$c/\text{\AA}$	13.3940(4)	13.3578(5)
$a/^\circ$	63.274(3)	63.364(3)
$b/^\circ$	88.730(2)	88.684(3)
$g/^\circ$	88.545(2)	88.508(3)
$V/\text{\AA}^3$	1323.47(8)	1317.01(8)
Z	2	2
$Z'$	1	1
Wavelength/ $\text{\AA}$	0.71073	0.71073
Radiation type	Mo $K\alpha$	Mo $K\alpha$
$\theta_{min}/^\circ$	1.702	1.706
$\theta_{max}/^\circ$	28.282	32.043
Measured Refl's.	13,613	17,246
Indep't Refl's	6556	8441
Refl's $I \geq 2\sigma(I)$	5914	6900
$R_{int}$	0.0189	0.0276
Parameters	414	407
Restraints	0	0
Largest Peak	0.687	0.951
Deepest Hole	-0.822	-0.920
Goof	1.055	1.035
$R_1$ (all data) <sup>a</sup>	0.0267	0.0449
$R_1$ <sup>a</sup>	0.0227	0.0323
$wR_2$ (all data) <sup>b</sup>	0.0538	0.0653
$wR_2$ <sup>b</sup>	0.0518	0.0605

<sup>a</sup>  $R_1 = \sum ||F_0| - |F_c|| / \sum |F_c|$ , <sup>b</sup>  $wR_2 = \{\sum [w(F_0^2 - F_c^2)^2] / \sum [w(F_0^2)^2]\}^{1/2}$ .

Crystallographic data for the structures reported in this contribution have been deposited with the Cambridge Crystallographic Data Centre as supplementary publication 2224921-224922. Copies of the data can be obtained free of charge on application to the CCDC, Cambridge, U.K. (<http://www.ccdc.cam.ac.uk/>).

### 2.3. Synthesis of $[Ln_2(tda)_3(H_2O)_5] \cdot 3H_2O$ ( $Ln = Sm$ (1), $Eu$ (2))

1.35 mmol (0.203 g) of  $H_2tda$  and 0.45 mmol of  $LnCl_3 \cdot 6H_2O$  (0.164 (1), 0.165 (2) g) were dissolved in 10 mL of water at room temperature with continuous stirring. Then, the pH of the solution was adjusted to ca. 3.3 with aqueous 0.5 M NaOH. If a small amount of a white solid remained at this point, it was filtered through paper and discarded. The clear solution was allowed to evaporate slowly. After 10 days, a crystalline material was formed, filtrated, washed with two portions of 1 mL of water, and air-dried. Some crystals were suitable for single-crystal X-ray diffraction analysis. Yield: 52% (1), 61% (2). Elemental analysis (%) Calcd. for 1,  $C_{12}H_{28}Sm_2O_{20}S_3$ : C, 16.21; H, 3.17; S, 10.82. Found: C, 16.55; H, 3.00; S, 11.09. Calcd. for 2,  $C_{12}H_{28}Eu_2O_{20}S_3$ : C, 16.15; H, 3.16; S, 10.78. Found: C, 16.42; H, 2.81; S, 11.03. Found: C, 16.42; H, 2.81; S, 11.45. IR (KBr,  $cm^{-1}$ ): main signals are almost identical for compounds 1 and 2: 3598(m), 3518(m), 3362(s), 2984(m), 2918(m), 1595(sh), 1564(vs), 1426(s), 1383(s), 1229(s), 1217(w), 1157(m), 1130(m), 962(w), 952(m), 918(m), 899(m), 733(m), 721(m), 710(m), 605(s), 463(m).

## 3. Results

### 3.1. Solution Studies

For a rational design of the synthetic procedure, the first step of the study was to look at the Ln(III)-tda systems in solution at room temperature and low ionic strength since previously reported data were not conclusive about the species formed, especially in the acid interval in which protonated species were detected by some authors but not by others (Table S1). Protonation equilibrium constants of the ligand (Table 2) were also redetermined under identical conditions: 0.15 mol·L<sup>-1</sup> NaClO<sub>4</sub> at 25.0 °C. The obtained results for the protonation constants are in total agreement with previous reports under similar conditions [65,73,74]. With these results and the previously reported hydrolysis constants of the Ln(III) ions under similar conditions [66], the stability constants of the species Ln(III)-tda were determined. This is also shown in Table 2. Only cationic species 1:1 ( $[Ln(tda)]^+$  and  $[Ln(Htda)]^{2+}$ ) and the anionic species 1:2 ( $[Ln(tda)_2]^-$ ) were detected in solution, with similar stability constant values for Sm(III) and Eu(III). It is interesting to compare the stability constants of tda species with those for oda and ida (some of them are also included in Table 2). A close inspection of log<sub>10</sub> K values shows that Ln(III)-tda species are much less stable than the analogous complexes with oda or ida. The change of O or N by S as a donor atom represents a loss of stability in the coordination compounds of lanthanide(III) ions.

**Table 2.** Logarithm of the acid-base and complexation equilibrium constants determined in this work in 0.15 mol·L<sup>-1</sup> NaClO<sub>4</sub> at 25.0 °C.  $H_2tda$  represents the fully protonated neutral form of thiodiacetic acid. Values given in parentheses are the 1σ statistical uncertainties in the last digit of the determined constant values. Selected stability constants for analogous oda and ida complexes (again,  $H_2oda$  and  $H_2ida$  represent the fully protonated neutral forms) were taken from selected reported data under similar experimental conditions.

Equilibrium	log <sub>10</sub> K	σ
$tda^{2-} + H^+ \rightarrow Htda^-$	4.23(1)	1.3
$tda^{2-} + 2H^+ \rightarrow H_2tda$	7.28(2)	
$Sm^{3+} + tda^{2-} \rightarrow [Sm(tda)]^+$	2.94(4)	0.7
$Sm^{3+} + 2tda^{2-} \rightarrow [Sm(tda)_2]^-$	5.16(6)	
$Sm^{3+} + H^+ + tda^{2-} \rightarrow [Sm(Htda)]^{2+}$	6.28(5)	

Table 2. Cont.

Equilibrium	$\log_{10} K$	$\sigma$
$\text{Eu}^{3+} + \text{tda}^{2-} \rightarrow [\text{Eu}(\text{tda})]^+$	3.06(1)	
$\text{Eu}^{3+} + 2\text{tda}^{2-} \rightarrow [\text{Eu}(\text{tda})_2]^-$	5.96(5)	0.4
$\text{Eu}^{3+} + \text{H}^+ + \text{tda}^{2-} \rightarrow [\text{Eu}(\text{Htda})]^{2+}$	5.7(2)	
oda		Ref.
$\text{Sm}^{3+} + \text{oda}^{2-} \rightarrow [\text{Sm}(\text{oda})]^+$	5.64	[75]
$\text{Sm}^{3+} + 2\text{oda}^{2-} \rightarrow [\text{Sm}(\text{oda})_2]^-$	9.62	[75]
$\text{Eu}^{3+} + \text{oda}^{2-} \rightarrow [\text{Eu}(\text{oda})]^+$	5.53	[76]
$\text{Eu}^{3+} + 2\text{oda}^{2-} \rightarrow [\text{Eu}(\text{oda})_2]^-$	10.04	[76]
ida		
$\text{Sm}^{3+} + \text{ida}^{2-} \rightarrow [\text{Sm}(\text{ida})]^+$	5.914	[14]
$\text{Sm}^{3+} + 2\text{ida}^{2-} \rightarrow [\text{Sm}(\text{ida})_2]^-$	10.230	[14]
$\text{Eu}^{3+} + \text{ida}^{2-} \rightarrow [\text{Eu}(\text{ida})]^+$	6.48	[77]
$\text{Eu}^{3+} + 2\text{ida}^{2-} \rightarrow [\text{Eu}(\text{ida})_2]^-$	11.65	[77]

Figure 1 shows the species distribution diagrams for Sm(III)-tda system built with these results for the ligand-to-metal molar ratios 1:1 and 3:1, while Figure S1 shows similar diagrams for Eu(III). The low stability of these complexes is reflected in the high percentage of free Ln(III), especially below pH 4–5. Even though the complex species  $[\text{Ln}(\text{Htda})]^{2+}$  is detected in this interval (contrary to what happens in oda or ida-containing systems), the partially protonated ligand gives place to a low-stability species that forms only in a relatively low percentage (the calculated  $\log_{10} K$  values for  $\text{Ln}^{3+} + \text{Htda}^- \rightarrow [\text{Ln}(\text{Htda})]^{2+}$  are 2.0 and 1.5 for Sm and Eu, respectively). It is worth mentioning at this point that the present results are in perfect agreement with previous findings based on the luminescence lifetime measurements of Eu(III) or Sm(III) ions in the presence of tda in an aqueous solution [78,79]. In particular, these findings suggest the non-participation of the S atom in the coordination sphere, which is in agreement with the formation of much less stable species in comparison to what happens with the analogous oda or ida ligands [78,79]. Besides, similar experiments carried out in the acid interval show the same average number of *ca.* six Sm-coordinated water molecules for conditions in which either  $[\text{Sm}(\text{tda})]^+$ ,  $[\text{Sm}(\text{Htda})]^{2+}$  or  $[\text{Sm}(\text{tda})(\text{Htda})]$  should predominate [78,80]. This accounts for the non-existence of the last species, which was not detected in this work. On the other hand, the hydrolysis of the lanthanide(III) ion at pH values above 7–8 represents a relevant competitive process to be considered in the synthesis of the compounds. In that sense, just above pH 3 and in the presence of ligand excess, mononuclear species are expected to be present. In contrast, the competition of hydrolysis processes is expected to be minimized.

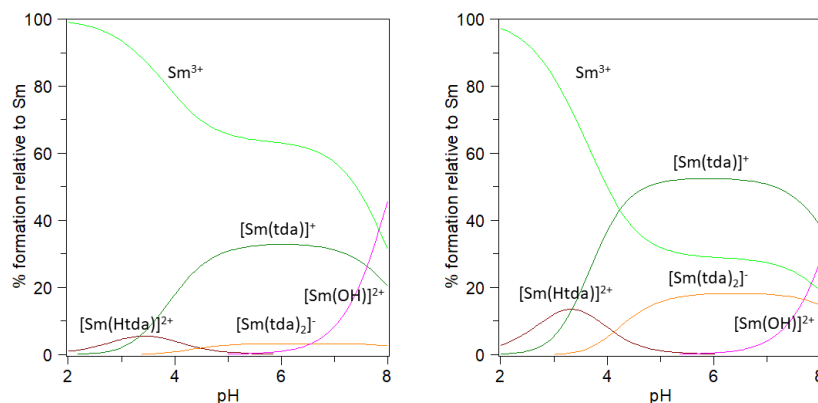


Figure 1. Species distribution diagram of the Sm-tda system at 25.0 °C,  $I = 0.15 \text{ mol}\cdot\text{L}^{-1} \text{ NaClO}_4$ . Left: total  $[\text{Sm}^{3+}] = 1 \text{ mM}$  and total  $[\text{tda}] = 1 \text{ mM}$ . Right: total  $[\text{Sm}^{3+}] = 1 \text{ mM}$  and total  $[\text{tda}] = 3 \text{ mM}$ .

### 3.2. Synthesis and Characterization

Following our previous strategy to isolate Ln complexes with ida and derivatives [19,81] and taking into account the results of the preceding section, we prepared the complexes  $[\text{Ln}_2(\text{tda})_3(\text{H}_2\text{O})_5]\cdot 3\text{H}_2\text{O}$  (Ln = Sm (1), Eu (2)). An aqueous solution of  $\text{LnCl}_3$  and  $\text{H}_2\text{tda}$  (molar ratio 1:3, pH 3.3) was allowed to evaporate slowly to obtain the crystalline compounds. Preliminary characterization of the solids by elemental analysis is in good agreement with the proposed formula. The IR spectra (Figure S2) were almost identical for both complexes suggesting very similar structures. It is noticeable the shift and splitting of the sharp signals  $\nu_s(\text{COO})$  ( $1698\text{ cm}^{-1}$ ) and  $\nu_{as}(\text{COO})$  ( $1430\text{ cm}^{-1}$ ) of the free ligand: **1** and **2** exhibit very strong  $\nu_s(\text{COO})$  signals at  $1595$  and  $1564\text{ cm}^{-1}$  and  $\nu_{as}(\text{COO})$  at  $1425$  and  $1383\text{ cm}^{-1}$ . The stoichiometric ratio found in the solids (molar ratio Ln:tda 2:3) is the same as found in the complexes  $[\text{Ln}_2(\text{tda})_3(\text{H}_2\text{O})_2]$  previously reported [57–59]. In those previous reports, the synthesis was performed by solvothermal procedures and, in general, in water: ethanol mixtures.

TGA of the solids (Figure S3) shows a broad weight loss up to  $200\text{ }^\circ\text{C}$ , corresponding to all the water molecules (calculated for **1**, 16.2%, found 15.2%; calculated for **2**, 16.2%, found 15.3%). Decomposition appears in both complexes at ca.  $320\text{ }^\circ\text{C}$ .

### 3.3. Crystal Structures

It was possible to obtain single crystals of **1** and **2**, which crystallize in the triclinic space group  $P\bar{1}$ . They are isostructural, so we will only discuss the structure of **1**. Selected bond lengths are presented in Table 3. Two crystallographically non-equivalent Sm atoms are present, both with coordination number nine (Figure 2). Sm1 atom is surrounded by seven carboxylic O atoms, one S atom (S1), and one O of a coordinated water molecule. Sm2 is bound to four O atoms from water molecules and five carboxylic O atoms arising from two different ligands (those containing the non-coordinated S2 and S3 atoms). Sm1–S1 distance is  $3.130(1)\text{ \AA}$ , which is close to the values found in similar structures containing Ln(III) ions and thiol-type S atoms (Table S2).

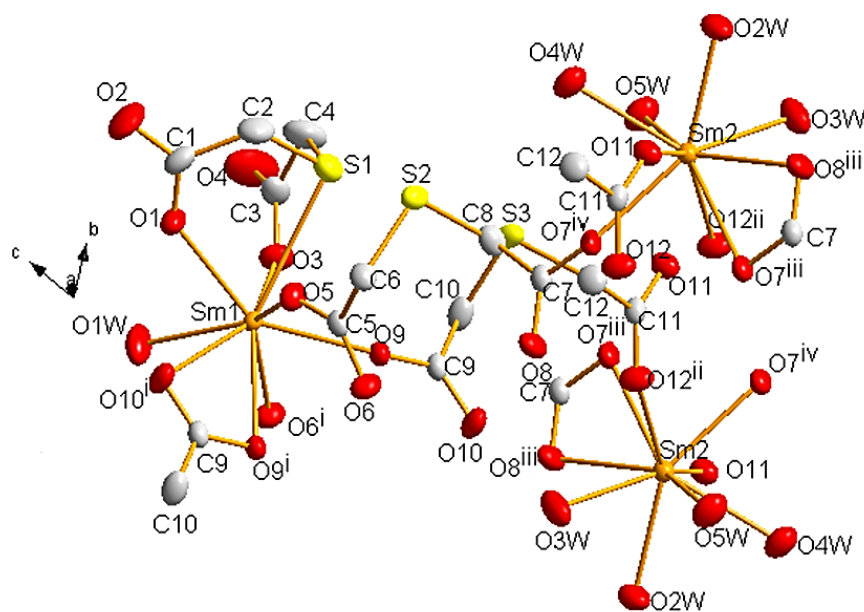


**Figure 2.** Perspective drawing of **1** showing the atom labels. Thermal ellipsoids are plotted at the 50% probability level. Hydrogen atoms and crystallization water molecules are omitted for clarity. Color code: Sm, orange; C, light grey; O, red; S, yellow. The symmetry-related atoms were obtained by applying the symmetry codes <sup>i</sup>  $1 - x, -y, 1 - z$ ; <sup>ii</sup>  $-x, 1 - y, -z$ ; <sup>iii</sup>  $1 - x, 1 - y, -z$ ; <sup>iv</sup>  $-1 + x, +y, +z$ .

**Table 3.** Bond lengths (Å) around central atom for **1** and **2**.

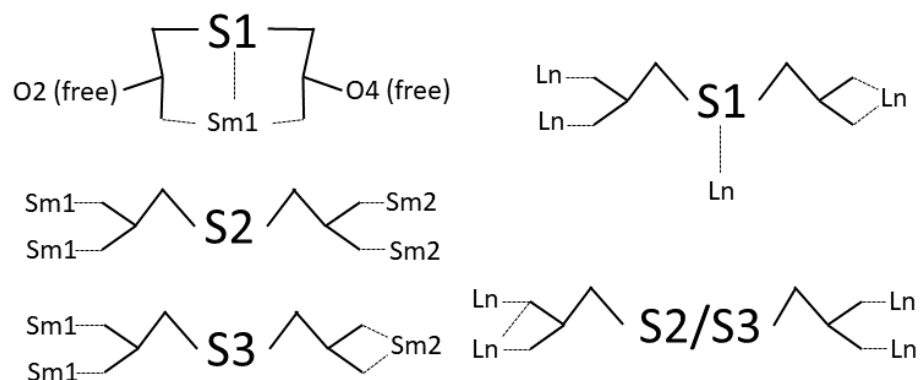
<b>1</b>				<b>2</b>			
Sm1-O9	2.392(2)	Sm2-O7 <sup>iii</sup>	2.596(2)	Eu1-O10 <sup>i</sup>	2.414(3)	Eu2-O11 <sup>iv</sup>	2.580(2)
Sm1-O9 <sup>i</sup>	2.585(2)	Sm2-O7 <sup>iv</sup>	2.410(2)	Eu1-O6 <sup>i</sup>	2.378(2)	Eu2-O8 <sup>ii</sup>	2.392(3)
Sm1-O6 <sup>i</sup>	2.428(2)	Sm2-O8 <sup>iii</sup>	2.552(2)	Eu1-O9	2.387(3)	Eu2-O11	2.394(2)
Sm1-O10 <sup>i</sup>	2.545(3)	Sm2-O11	2.400(2)	Eu1-O5	2.539(3)	Eu2-O7 <sup>iii</sup>	2.405(3)
Sm1-O1	2.376(2)	Sm2-O12 <sup>ii</sup>	2.413(2)	Eu1-O1	2.362(3)	Eu2-O12 <sup>ii</sup>	2.544(3)
Sm1-O5	2.396(2)	Sm2-O2W	2.433(3)	Eu1-O3	2.361(3)	Eu2-O5W	2.420(3)
Sm1-O3	2.376(2)	Sm2-O3W	2.438(2)	Eu1-O6	2.570(3)	Eu2-O2W	2.444(3)
Sm1-O1W	2.427(3)	Sm2-O5W	2.456(2)	Eu1-O1W	2.423(3)	Eu2-O4W	2.503(3)
Sm1-S1	3.130(1)	Sm2-O4W	2.520(3)	Eu1-S1	3.126(1)	Eu2-O3W	2.427(3)

<sup>i</sup> 1 - x, -y, 1 - z; <sup>ii</sup> -x, 1 - y, -z; <sup>iii</sup> 1 - x, 1 - y, -z; <sup>iv</sup> -1 + x, +y, +z

<sup>i</sup> 1 - x, 2 - y, 1 - z; <sup>ii</sup> -x, 2 - y, 1 - z; <sup>iii</sup> x, -1 + y, 1 + z; <sup>iv</sup> -x, 1 - y, 2 - z

In both Sm ions, polyhedra can be described as a tricapped trigonal prism (JTCTPR-9) [82,83]. For Sm1, the tricapped trigonal prism is quite irregular with O1, O3, O5, O9, O6i, and O10i as the vertices of the prism (average distance 2.419 Å), and OW1, O9i, and S1 in the apices (average distance 2.714 Å). In the case of Sm2, O2W, O3W, O4W, O11, O7iii, and O12ii conform the prism (average distance 2.467 Å), while O5W, O7iv, and O8iii occupy the apical positions (average distance 2.473 Å). This is shown in Figure S4.

It is interesting to view the connection between Sm(III) ions provided by the ligand (Scheme 1). Three non-equivalent ligands are present in the structure. Tda residue containing S1 does not link Sm ions. On the contrary, it is only bound to Sm1 as a tridentate ligand, generating two O atoms (O2 and O6) that do not participate in the coordination. The ligand with S2 connects four Sm ions in a monodentate fashion. The third ligand (with S3) connects three Sm(III) ions, bis-monodentate towards Sm1 and bidentate towards Sm2.



**Scheme 1.** Coordination modes of tda in compound **1** (left) and in previously reported structures  $[\text{Ln}_2(\text{tda})_3(\text{H}_2\text{O})_2]$  (right) [59–61].

The coordinative versatility of this ligand provokes the formation of thick sheets in the bc plane (Figure 3). Sm1 polyhedra are disposed of in couples sharing an edge through carboxylate groups of ligands with S2 and S3. In contrast, the Sm2 polyhedron shares an edge with an Sm1 polyhedron through O atoms from the third ligand (with S3).

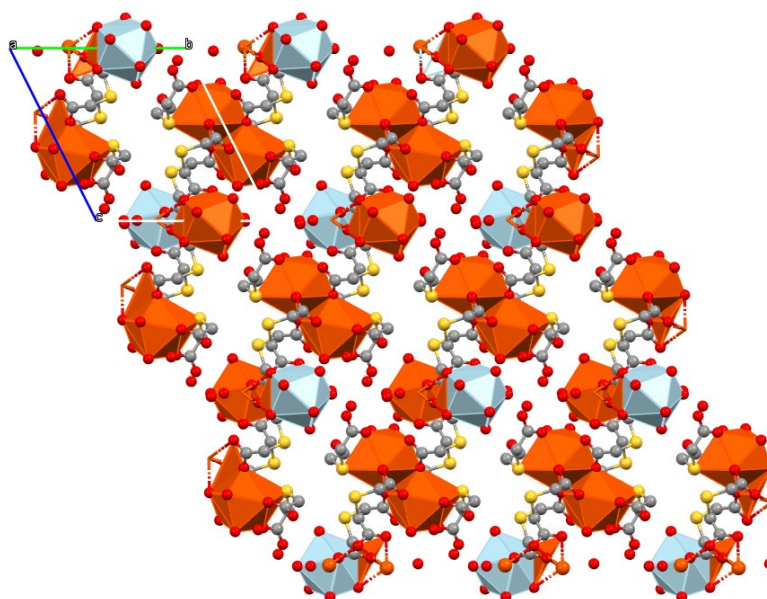


**Figure 3.** Packing of **1** in the bc plane. Polyhedra of Sm1 are colored orange, while Sm2 ones are light blue. Hydrogen atoms and crystallization water molecules are omitted for clarity.

Crystallization water molecules occupy the free space between the sheets and are involved in H-bonds, in particular with the uncoordinated O atoms. This is shown in Figure S5.

Previously reported structures with formula  $[\text{Ln}_2(\text{tda})_3(\text{H}_2\text{O})_2]$  exhibit the identical molar ratio Ln:tda found in **1** and **2** [59–61]. They crystallize in the same triclinic space group  $\text{P}\bar{1}$ , contain two crystallographically non-equivalent Ln atoms, and also present a 2D structure. It is interesting to compare the Ln-S distances. They are 3.105 and 3.091 Å for Dy [59,60], 3.105 Å for Eu [61], 3.098 Å for Gd [60], 3.122 Å for Sm [59], and 3.099 Å for Tb [60]. These values have not been considered as a bond distance, except in the Eu structure. Assuming that an Ln-S bond is present, Ln1 is coordinated by eight oxygen atoms (all of them from carboxylate groups) and one sulfur atom, and Ln2 is coordinated by nine O atoms, two of them from coordinated water molecules. From the ligand point of view, two coordination modes are present, as shown in Scheme 1.

### 3.4. Photophysical Studies

Figure 4 depicts the solid-state luminescence spectra of compound **2** upon direct excitation of Eu(III) ion at 394 nm, selected from the excitation spectrum and giving place to the characteristic emission profile of the intra-configuration emission of the metal ion. Eu(III) is, in general, a much more intense luminescence emitter than Sm(III) [84], accounting for compound **2** is a much more intense emitter than compound **1** (which is shown in Figure S6, together with the excitation spectra and the assignment for emission bands). The emission spectra of Eu(III) show the characteristic five main bands corresponding to the intra-configuration transitions  $^5\text{D}_0 \rightarrow ^7\text{F}_J$ , with  $J = 0-4$ . Noticeably, the truly forbidden transition  $^5\text{D}_0 \rightarrow ^7\text{F}_0$  is observed, even though with very low intensity. This band is probably associated with the less-symmetric Eu1 center (bound S1 atom) described in the crystal structure. The presence of the S1 atom in one of the apices of the tricapped trigonal prism excludes the existence of a mirror plane orthogonal to the main symmetry axis [85,86]. Indeed, in the  $[\text{Eu}(\text{oda})_3]^{3-}$  complex, with all positions of the tricapped trigonal prism occupied O atoms and similar Eu-O bond distances, this forbidden band is not observed [18]. The magnetic dipole transition  $^5\text{D}_0 \rightarrow ^7\text{F}_1$  band shows in compound **2** an intense degenerated profile, in line with the rotational symmetry in the coordination geometry. Furthermore, the  $^5\text{D}_0 \rightarrow ^7\text{F}_2$  hypersensitive band is 1.3 times more intense than the magnetic dipole transition  $^5\text{D}_0 \rightarrow ^7\text{F}_1$  band. Noticeably, in the previously reported

complex  $[\text{Eu}_2(\text{tda})_3(\text{H}_2\text{O})_2]$ , with just two coordinated water molecules coordinated to one of the emissive centers, the  $^5\text{D}_0 \rightarrow ^7\text{F}_2$  hypersensitive band shows an intensity more than three times higher than that of the  $^5\text{D}_0 \rightarrow ^7\text{F}_1$  band [61]. The presence of four coordinated water molecules in **2** accounts for the lower comparative observed intensity of the  $^5\text{D}_0 \rightarrow ^7\text{F}_2$  band. Also in line with this, the behavior of compound **1** is also influenced by the presence of coordinated water molecules, which diminishes the emissive behavior of Sm ion, relative to that observed for  $[\text{Sm}_2(\text{tda})_3(\text{H}_2\text{O})_2]$  [59] (Figure S6).

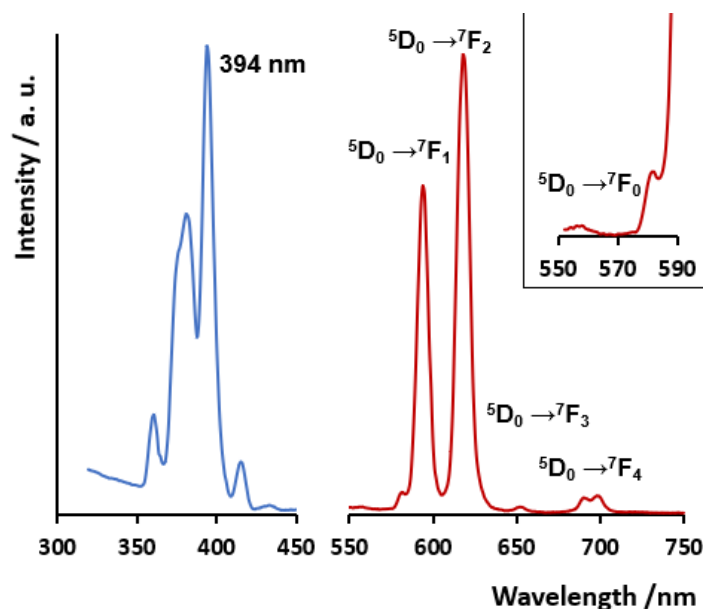


**Figure 4.** (Left): solid-state excitation spectra. (Right): emission spectra of compound **2** excited at 394 nm. Transitions assigned to each band are also shown. An inset is included for more detail on the  $^5\text{D}_0 \rightarrow ^7\text{F}_0$  band.

#### 4. Conclusions

The chemistry of thiodiacetato with the lanthanide ions Sm(III) and Eu(III) has been explored. First, the solution behavior of this system has been studied, and some light has been shed on the formed species, considering also previously reported inconclusive findings. Starting from this knowledge, two new compounds have been obtained and fully characterized, showing the versatility of the thiodiacetato ligand, which can either chelate or connect the lanthanide(III) centers. The solid-state optical properties of the two compounds were studied, the Eu(III) compound resulting in a better luminescence emitter material.

**Supplementary Materials:** The following supporting information can be downloaded at: <https://www.mdpi.com/article/10.3390/cryst13010056/s1>, Figure S1: Species distribution diagram of the Eu-tda system at 25.0 °C,  $I = 0.15 \text{ mol}\cdot\text{L}^{-1} \text{ NaClO}_4$ ; Figure S2: IR spectra of complexes **1** and **2**, together with the protonated ligand; Figure S3: TGA diagram of compounds **1** and **2** under nitrogen atmosphere; Figure S4: Polyhedra around the Sm(III) ions in **1**; Figure S5: Packing of **1** in the *bc* plane showing H-bonds; Figure S6: solid-state excitation and emission spectra of compound **1**; Table S1: Previously potentiometrically determined stability constant values for Sm and Eu complexes with tda; Table S2: Typical bond distances Ln-S found in structures containing Ln(III) ions and thiol ligands.

**Author Contributions:** Conceptualization, C.K.; synthesis and characterization, C.K.; potentiometric studies, J.T.; photophysical studies, J.T.; diffraction studies, J.G.-P.; writing—original draft preparation, C.K. and J.T.; writing—review and editing, C.K., J.T. and J.G.-P. All authors have read and agreed to the published version of the manuscript.

**Funding:** This research received no external funding.

**Data Availability Statement:** Not applicable.

**Acknowledgments:** We are grateful for the financial support from the Uruguayan organizations CSIC (Comisión Sectorial de Investigación Científica) by Programa de Apoyo a Grupos de Investigación and PEDECIBA (Programa para el Desarrollo de las Ciencias Básicas). This work has also been partially supported by MCIN/AEI/10.13039/5011000011033 in the project PID2019-106383GB-C44. J.G.-P. thanks to Servicios Generales de Apoyo a la Investigación (SEGAI) at La Laguna University.

**Conflicts of Interest:** The authors declare no conflict of interest.

## References

1. Murugesu, M.; Schelter, E.J. Not Just Lewis Acids: Preface for the Forum on New Trends and Applications for Lanthanides. *Inorg. Chem.* **2016**, *55*, 9951–9953. [[CrossRef](#)] [[PubMed](#)]
2. Cotton, S.A.; Raithby, P.R. Systematics and Surprises in Lanthanide Coordination Chemistry. *Coord. Chem. Rev.* **2017**, *340*, 220–231. [[CrossRef](#)]
3. Chundawat, N.S.; Jadoun, S.; Zarrintaj, P.; Chauhan, N.P.S. Lanthanide Complexes as Anticancer Agents: A Review. *Polyhedron* **2021**, *207*, 115387. [[CrossRef](#)]
4. Bao, G. Lanthanide Complexes for Drug Delivery and Therapeutics. *J. Lumin.* **2020**, *228*, 117622. [[CrossRef](#)]
5. Zheng, Z.; Lu, H.; Wang, Y.; Bao, H.; Li, Z.-J.; Xiao, G.-P.; Lin, J.; Qian, Y.; Wang, J.-Q. Tuning of the Network Dimensionality and Photoluminescent Properties in Homo- and Heteroleptic Lanthanide Coordination Polymers. *Inorg. Chem.* **2021**, *60*, 1359–1366. [[CrossRef](#)]
6. Zhang, P.; Guo, Y.-N.; Tang, J. Recent Advances in Dysprosium-Based Single Molecule Magnets: Structural Overview and Synthetic Strategies. *Coord. Chem. Rev.* **2013**, *257*, 1728–1763. [[CrossRef](#)]
7. Jin, J.; Xue, J.; Liu, Y.; Yang, G.; Wang, Y.-Y. Recent Progresses in Luminescent Metal–Organic Frameworks (LMOFs) as Sensors for the Detection of Anions and Cations in Aqueous Solution. *Dalton Trans.* **2021**, *50*, 1950–1972. [[CrossRef](#)]
8. Huangfu, M.; Wang, M.; Lin, C.; Wang, J.; Wu, P. Luminescent Metal–Organic Frameworks as Chemical Sensors Based on “Mechanism–Response”: A Review. *Dalton Trans.* **2021**, *50*, 3429–3449. [[CrossRef](#)]
9. Kremer, C.; Torres, J.; Domínguez, S. Lanthanide Complexes with Oda, Ida, and Nta: From Discrete Coordination Compounds to Supramolecular Assemblies. *J. Mol. Struct.* **2008**, *879*, 130–149. [[CrossRef](#)]
10. Wen, Y.-H.; Wu, X.-H.; Bi, S.; Zhang, S.-S. Synthesis and Structural Characterization of Lanthanide Oxalate–Oxydiacetate Mixed-Ligand Coordination Polymers  $\{[\text{Ln}(\text{Oda})(\text{H}_2\text{O})_x]_2(\text{Ox})\}_n$  ( $x = 3$  for Ln = La, Ce, Pr, Gd, Tb and  $x = 2$  for Ln = Er). *J. Coord. Chem.* **2009**, *62*, 1249–1259. [[CrossRef](#)]
11. Lennartson, A.; Håkansson, M. Total Spontaneous Resolution of Nine-Coordinate Complexes. *CrystEngComm* **2009**, *11*, 1979. [[CrossRef](#)]
12. Zhou, Q.; Yang, F.; Liu, D.; Peng, Y.; Li, G.; Shi, Z.; Feng, S. Synthesis, Structures, and Magnetic Properties of Three Fluoride-Bridged Lanthanide Compounds: Effect of Bridging Fluoride Ions on Magnetic Behaviors. *Inorg. Chem.* **2012**, *51*, 7529–7536. [[CrossRef](#)] [[PubMed](#)]
13. Ma, J.; Ma, T.; Qian, R.; Zhou, L.; Guo, Q.; Yang, J.-H.; Yang, Q. Na–Ln Heterometallic Coordination Polymers: Structure Modulation by  $\text{Na}^+$  Concentration and Efficient Detection of Tetracycline Antibiotics and 4-(Phenylazo)Aniline. *Inorg. Chem.* **2021**, *60*, 7937–7951. [[CrossRef](#)]
14. Torres, J.; Kremer, C.; Domínguez, S. Chemical Speciation of Polynuclear Complexes Containing  $[\text{Ln}_2\text{M}_3\text{L}_6]$  Units. *Pure Appl. Chem.* **2008**, *80*, 1303–1316. [[CrossRef](#)]
15. Cancino, P.; Santibañez, L.; Stevens, C.; Fuentealba, P.; Audebrand, N.; Aravena, D.; Torres, J.; Martínez, S.; Kremer, C.; Spodine, E. Influence of the Channel Size of Isostructural 3d–4f MOFs on the Catalytic Aerobic Oxidation of Cycloalkenes. *New J. Chem.* **2019**, *43*, 11057–11064. [[CrossRef](#)]
16. Santibañez, L.; Escalona, N.; Torres, J.; Kremer, C.; Cancino, P.; Spodine, E. CuII- and CoII-Based MOFs:  $\{[\text{La}_2\text{Cu}_3(\mu\text{-H}_2\text{O})(\text{ODA})_6(\text{H}_2\text{O})_3] \cdot 3\text{H}_2\text{O}\}_n$  and  $\{[\text{La}_2\text{Co}_3(\text{ODA})_6(\text{H}_2\text{O})_6] \cdot 12\text{H}_2\text{O}\}_n$ . The Relevance of Physicochemical Properties on the Catalytic Aerobic Oxidation of Cyclohexene. *Catalysts* **2020**, *10*, 589. [[CrossRef](#)]
17. Igoa, F.; Peinado, G.; Suescun, L.; Kremer, C.; Torres, J. Design of a White-Light Emitting Material Based on a Mixed-Lanthanide Metal Organic Framework. *J. Solid State Chem.* **2019**, *279*, 120925. [[CrossRef](#)]
18. Igoa, F.; Romero, M.; Peinado, G.; Castiglioni, J.; González-Platas, J.; Faccio, R.; Suescun, L.; Kremer, C.; Torres, J. Ln(III)–Ni(II) Heteropolynuclear Metal Organic Frameworks of Oxydiacetate with Promising Proton-Conductive Properties. *CrystEngComm* **2020**, *22*, 5638–5648. [[CrossRef](#)]
19. Kremer, C.; Morales, P.; Torres, J.; Castiglioni, J.; González-Platas, J.; Hummert, M.; Schumann, H.; Domínguez, S. Novel Lanthanide–Iminodiacetate Frameworks with Hexagonal Pores. *Inorg. Chem. Commun.* **2008**, *11*, 862–864. [[CrossRef](#)]
20. Bonomo, R.P.; Rizzarelli, E.; Bresciani-Pahor, N.; Nardin, G. Properties and X-Ray Crystal Structures of Copper(II) Mixed Complexes with Thiodiacetate and 2,2'-Bipyridyl or 2,2':6'2"-Terpyridyl. *J. Chem. Soc. Dalton Trans.* **1982**, 681–685. [[CrossRef](#)]
21. Alarcón-Payer, C.; Pivetta, T.; Choquesillo-Lazarte, D.; González-Pérez, J.M.; Crisponi, G.; Castiñeiras, A.; Niclós-Gutiérrez, J. Thiodiacetate-Copper(II) Chelates with or without N-Heterocyclic Donor Ligands: Molecular and/or Crystal Structures of  $[\text{Cu}(\text{Tda})]_n$ ,  $[\text{Cu}(\text{Tda})(\text{Him})_2(\text{H}_2\text{O})]$  and  $[\text{Cu}(\text{Tda})(5\text{Mphen})] \cdot 2\text{H}_2\text{O}$  (Him=imidazole, 5Mphen=5-Methyl-1,10-Phenanthroline). *Inorg. Chim. Acta* **2005**, *358*, 1918–1926. [[CrossRef](#)]

22. Abbaszadeh, A.; Safari, N.; Amani, V.; Notash, B.; Raei, F.; Eftekhari, F. Mononuclear and Dinuclear Copper(II) Complexes Containing N, O and S Donor Ligands: Synthesis, Characterization, Crystal Structure Determination and Antimicrobial Activity of  $[\text{Cu}(\text{Phen})(\text{Tda})]\cdot 2\text{H}_2\text{O}$  and  $[(\text{Phen})_2\text{Cu}(\mu\text{-Tda})\text{Cu}(\text{Phen})](\text{ClO}_4)_2\cdot 1.5\text{H}_2\text{O}$ . *Iran. J. Chem. Chem. Eng. IJCCE* **2014**, *33*, 1–33. [[CrossRef](#)]
23. Patel, D.K.; Choquesillo-Lazarte, D.; Domínguez-Martín, A.; Brandi-Blanco, M.P.; González-Pérez, J.M.; Castiñeiras, A.; Niclós-Gutiérrez, J. Chelating Ligand Conformation Driving the Hypoxanthine Metal Binding Patterns. *Inorg. Chem.* **2011**, *50*, 10549–10551. [[CrossRef](#)] [[PubMed](#)]
24. Kopel, P.; Trávníček, Z.; Marek, J.; Mrozinski, J. Syntheses and Study on Nickel(II) Complexes with Thiodiglycolic Acid and Nitrogen-Donor Ligands. X-Ray Structures of  $[\text{Ni}(\text{Bpy})(\text{Tdga})(\text{H}_2\text{O})]\cdot 4\text{H}_2\text{O}$  and  $[(\text{En})\text{Ni}(\mu\text{-Tdga})_2\text{Ni}(\text{En})]\cdot 4\text{H}_2\text{O}$  ( $\text{TdgaH}_2 = \text{thiodiglycolic Acid}$ ). *Polyhedron* **2004**, *23*, 1573–1578. [[CrossRef](#)]
25. Wang, Y.-L.; Chang, G.-J.; Liu, B.-X. Aqua(2,2'-Diamino-4,4'-Bi-1,3-Thiazole- $\kappa^2 N^3, N^3$ ')(Thiodiacetato- $\kappa^3 O, S, O'$ )Nickel(II) Monohydrate. *Acta Crystallogr. Sect. E Struct. Rep. Online* **2011**, *67*, m681. [[CrossRef](#)]
26. Pan, T.-T.; Su, J.-R.; Xu, D.-J. Hexaaquanickelate(II) Bis(Thiodiacetato- $\kappa^3 O, S, O'$ )Nickel(II) Tetrahydrate. *Acta Crystallogr. Sect. E Struct. Rep. Online* **2005**, *61*, m1376–m1378. [[CrossRef](#)]
27. Alarcón-Payer, C.; Pivetta, T.; Choquesillo-Lazarte, D.; González-Pérez, J.M.; Crisponi, G.; Castiñeiras, A.; Niclós-Gutiérrez, J. Structural Correlations in Nickel(II)-Thiodiacetato Complexes: Molecular and Crystal Structures and Properties of  $[\text{Ni}(\text{Tda})(\text{H}_2\text{O})_3]$ . *Inorg. Chem. Commun.* **2004**, *7*, 1277–1280. [[CrossRef](#)]
28. Pan, T.-T.; Su, J.-R.; Xu, D.-J. Tris(1H-Imidazole- $\kappa N^3$ ')(Thiodiacetato- $\kappa^3 O, S, O'$ )Nickel(II) Monohydrate. *Acta Crystallogr. Sect. E Struct. Rep. Online* **2005**, *61*, m1576–m1578. [[CrossRef](#)]
29. Delaunay, J.; Kappenstein, C.; Hugel, R. Structure Cristalline et Moléculaire Du Bis-Thio(Diacétato)Nickelate(II) de Potassium Trihydraté. *Acta Crystallogr. B* **1976**, *32*, 2341–2345. [[CrossRef](#)]
30. Cao, L.; Liu, J.-G.; Xu, D.-J. Tris(1H-Benzimidazole- $\kappa N^3$ ')(Thiodiacetato- $\kappa^3 O, S, O'$ )Cobalt(II) Dihydrate. *Acta Crystallogr. Sect. E Struct. Rep. Online* **2006**, *62*, m579–m581. [[CrossRef](#)]
31. Liu, B.-X.; Yu, J.-Y.; Xu, D.-J. Aqua(2,2'-Diamino-4,4'-Bi-1,3-Thiazole- $\kappa^2 N, N'$ ')(Thiodiacetato- $\kappa^3 O, S, O'$ )Cobalt(II) Dihydrate. *Acta Crystallogr. Sect. E Struct. Rep. Online* **2005**, *61*, m1978–m1980. [[CrossRef](#)]
32. Korchagin, D.V.; Gureev, Y.E.; Yureva, E.A.; Shilov, G.V.; Akimov, A.V.; Misochko, E.Y.; Morgunov, R.B.; Zakharov, K.V.; Vasiliev, A.N.; Palii, A.V.; et al. Field-Induced Single-Ion Magnet Based on a Quasi-Octahedral Co(II) Complex with Mixed Sulfur-Oxygen Coordination Environment. *Dalton Trans.* **2021**, *50*, 13815–13822. [[CrossRef](#)] [[PubMed](#)]
33. Grirrane, A.; Pastor, A.; Álvarez, E.; Mealli, C.; Ienco, A.; Masi, D.; Galindo, A. Thiodiacetate Cobalt(II) Complexes: Synthesis, Structure and Properties. *Inorg. Chem. Commun.* **2005**, *8*, 463–466. [[CrossRef](#)]
34. Grirrane, A.; Pastor, A.; Álvarez, E.; Mealli, C.; Ienco, A.; Rosa, P.; Galindo, A. Thiodiacetate and Oxydiacetate Cobalt Complexes: Synthesis, Structure and Stereochemical Features. *Eur. J. Inorg. Chem.* **2007**, *2007*, 3543–3552. [[CrossRef](#)]
35. Wang, H.; Gao, S.; Ng, S.W. Hexaaquacobalt(II) Bis(2,2'-Sulfanediyldiacetato- $\kappa^3 O, S, O'$ )Cobaltate(II) Tetrahydrate. *Acta Crystallogr. Sect. E Struct. Rep. Online* **2011**, *67*, m1521. [[CrossRef](#)] [[PubMed](#)]
36. Wu, J.-Y.; Xie, L.-M.; He, H.-Y.; Zhou, X.; Zhu, L.-G. Aqua(1,10-Phenanthroline)(Thiodiglycolato)Cobalt(II). *Acta Crystallogr. Sect. E Struct. Rep. Online* **2005**, *61*, m568–m570. [[CrossRef](#)]
37. Grirrane, A.; Pastor, A.; Galindo, A.; Álvarez, E.; Mealli, C.; Ienco, A.; Orlandini, A.; Rosa, P.; Caneschi, A.; Barra, A.; et al. Thiodiacetate-Manganese Chemistry with N Ligands: Unique Control of the Supramolecular Arrangement over the Metal Coordination Mode. *Chem. Eur. J.* **2011**, *17*, 10600–10617. [[CrossRef](#)]
38. Drew, M.G.B.; Rice, D.A.; Timewell, C.W. Crystal and Molecular Structure of Triaquazinc(II) Thiodiglycolate Monohydrate. *J. Chem. Soc. Dalton Trans.* **1975**, 144–148. [[CrossRef](#)]
39. Baggio, R.; Pereg, M.; Garland, M.T. Aqua(2,2'-Bipyridyl-N,N')(Thiodiacetato-O,O',S)Zinc(II) Tetrahydrate. *Acta Crystallogr. C* **1996**, *52*, 2457–2460. [[CrossRef](#)]
40. Arıcı, M.; Yeşilel, O.Z.; Acar, E.; Dege, N. Synthesis, Characterization and Properties of Nicotinamide and Isonicotinamide Complexes with Diverse Dicarboxylic Acids. *Polyhedron* **2017**, *127*, 293–301. [[CrossRef](#)]
41. Pan, T.-T.; Xu, D.-J. Tris(1H-Benzimidazole- $\kappa N^3$ ')(Thiodiacetato- $\kappa^3 O, S, O'$ )Cadmium(II) Dihydrate. *Acta Crystallogr. Sect. E Struct. Rep. Online* **2005**, *61*, m1735–m1737. [[CrossRef](#)]
42. Grirrane, A.; Pastor, A.; Álvarez, E.; Galindo, A. Magnesium Dicarboxylates: First Structurally Characterized Oxydiacetate and Thiodiacetate Magnesium Complexes. *Inorg. Chem. Commun.* **2005**, *8*, 453–456. [[CrossRef](#)]
43. Shan, X.; Ellern, A.; Guzei, I.A.; Espenson, J.H. Syntheses and Oxidation of Methyloxorhenium(V) Complexes with Tridentate Ligands. *Inorg. Chem.* **2003**, *42*, 2362–2367. [[CrossRef](#)] [[PubMed](#)]
44. Álvarez, L.; Grirrane, A.; Moyano, R.; Álvarez, E.; Pastor, A.; Galindo, A. Comparison of the Coordination Capabilities of Thiodiacetate and Oxydiacetate Ligands through the X-Ray Characterization and DFT Studies of  $[\text{V}(\text{O})(\text{Tda})(\text{Phen})]\cdot 4\text{H}_2\text{O}$  and  $[\text{V}(\text{O})(\text{Oda})(\text{Phen})]\cdot 1.5\text{H}_2\text{O}$ . *Polyhedron* **2010**, *29*, 3028–3035. [[CrossRef](#)]
45. Zangl, A.; Klüfers, P.; Schaniel, D.; Woike, T. Photoinduced Linkage Isomerism of  $\{\text{RuNO}\}_6$  Complexes with Bioligands and Related Chelators. *Dalton Trans.* **2009**, 1034–1045. [[CrossRef](#)] [[PubMed](#)]
46. Marek, J.; Trávníček, Z.; Kopel, P. Diaquabis(1,10-Phenanthroline- $\kappa^2 N, N'$ )Manganese(II) Thiodiglycolate Bis(1,10-Phenanthroline- $\kappa^2 N, N'$ ')(Thiodiglycolato- $\kappa^2 O, O'$ )Manganese(II) Tridecahydrate. *Acta Crystallogr. C* **2003**, *59*, m429–m431. [[CrossRef](#)]

47. Wang, L.; Shan, Y.; Gu, X.; Ni, L.; Zhang, W. Assembly and Photocatalysis of Three Novel Metal–Organic Frameworks Tuned by Metal Polymeric Motifs. *J. Coord. Chem.* **2015**, *68*, 2014–2028. [[CrossRef](#)]
48. Baggio, R.; Garland, M.T.; Manzur, J.; Peña, O.; Perec, M.; Spodine, E.; Vega, A. A Dinuclear Copper(II) Complex Involving Monoatomic O-Carboxylate Bridging and Cu–S(Thioether) Bonds: [Cu(Tda)(Phen)]<sub>2</sub>·H<sub>2</sub>tada (Tda=thiodiacetate, Phen=phenanthroline). *Inorg. Chim. Acta* **1999**, *286*, 74–79. [[CrossRef](#)]
49. Ahmad, M.S.; Khalid, M.; Khan, M.S.; Shahid, M.; Ahmad, M.; Monika; Ansari, A.; Ashafaq, M. Exploring Catecholase Activity in Dinuclear Mn(II) and Cu(II) Complexes: An Experimental and Theoretical Approach. *New J. Chem.* **2020**, *44*, 7998–8009. [[CrossRef](#)]
50. Kopel, P.; Trávníček, Z.; Marek, J.; Korabik, M.; Mrozinski, J. Syntheses and Properties of Binuclear Copper(II) Mixed-Ligand Complexes Involving Thiodiglycolic Acid. *Polyhedron* **2003**, *22*, 411–418. [[CrossRef](#)]
51. Grirrane, A.; Pastor, A.; Galindo, A.; del Río, D.; Orlandini, A.; Mealli, C.; Ienco, A.; Caneschi, A.; Fernández Sanz, J. Supramolecular Interactions as Determining Factors of the Geometry of Metallic Building Blocks: Tetracarboxylate Dimanganese Species. *Angew. Chem. Int. Ed.* **2005**, *44*, 3429–3432. [[CrossRef](#)] [[PubMed](#)]
52. Neuman, N.I.; Burna, E.; Baggio, R.; Passeggi, M.C.G.; Rizzi, A.C.; Brondino, C.D. Transition from Isolated to Interacting Copper(II) Pairs in Extended Lattices Evaluated by Single Crystal EPR Spectroscopy. *Inorg. Chem. Front.* **2015**, *2*, 837–845. [[CrossRef](#)]
53. Grirrane, A.; Pastor, A.; Álvarez, E.; Mealli, C.; Ienco, A.; Galindo, A. Novel Results on Thiodiacetate Zinc(II) Complexes: Synthesis and Structure of [Zn(Tda)(Phen)]<sub>2</sub>·5H<sub>2</sub>O. *Inorg. Chem. Commun.* **2006**, *9*, 160–163. [[CrossRef](#)]
54. Sun, D.; Xu, M.-Z.; Liu, S.-S.; Yuan, S.; Lu, H.-F.; Feng, S.-Y.; Sun, D.-F. Eight Zn(II) Coordination Networks Based on Flexible 1,4-Di(1H-Imidazol-1-yl)butane and Different Dicarboxylates: Crystal Structures, Water Clusters, and Topologies. *Dalton Trans.* **2013**, *42*, 12324. [[CrossRef](#)]
55. Packiaraj, S.; Kanchana, P.; Pushpaveni, A.; Puschmann, H.; Govindarajan, S. Different Coordination Geometries of Lighter Lanthanates Driven by the Symmetry of Guanidines as Charge Compensators. *New J. Chem.* **2019**, *43*, 979–991. [[CrossRef](#)]
56. Malmberg, T.; Oskarsson, Å.; Rømming, C.; Gronowitz, S.; Koskikallio, J.; Swahn, C.-G. Structural Studies on the Rare Earth Carboxylates. 22. The Crystal Structure of Tetra-Aquo-Thiodiacetate neodymium(III) Chloride. *Acta Chem. Scand.* **1973**, *27*, 2923–2929. [[CrossRef](#)]
57. Kepert, C.J.; Skelton, B.W.; White, A.H. Structural Systematics of Rare Earth Complexes. XXI Polymeric Sodium Bis(Thiodiglycolato)Neodymium(III). *Aust. J. Chem.* **1999**, *52*, 617. [[CrossRef](#)]
58. Ghadermazi, M.; Olmstead, M.M.; Rostami, S.; Attar Gharamaleki, J. Poly[[Piperazine-1,4-Dium [Diaquatetrakis(μ-Sulfanediyldiacetato)Dicerate(III)]] Trihydrate]. *Acta Crystallogr. Sect. E Struct. Rep. Online* **2011**, *67*, m291–m292. [[CrossRef](#)]
59. Hou, X.; Li, D.; Wang, X.; Wang, J.; Ren, Y.; Zhang, M. Syntheses, Structures and Luminescence Properties of Ln-Coordination Polymers Based on Flexible Thiodiacetic Acid Ligand. *Chin. J. Chem.* **2009**, *27*, 1481–1486. [[CrossRef](#)]
60. Wen, H.-R.; Dong, P.-P.; Liang, F.-Y.; Liu, S.-J.; Xie, X.-R.; Tang, Y.-Z. A Family of 2D Lanthanide Complexes Based on Flexible Thiodiacetic Acid with Magnetocaloric or Ferromagnetic Properties. *Inorg. Chim. Acta* **2017**, *455*, 190–196. [[CrossRef](#)]
61. Wang, H.-S.; Bao, W.-J.; Ren, S.-B.; Chen, M.; Wang, K.; Xia, X.-H. Fluorescent Sulfur-Tagged Europium(III) Coordination Polymers for Monitoring Reactive Oxygen Species. *Anal. Chem.* **2015**, *87*, 6828–6833. [[CrossRef](#)] [[PubMed](#)]
62. Hosseinabadi, F.; Ghadermazi, M.; Taran, M.; Derikvand, Z. Synthesis, Crystal Structure, Spectroscopic, Thermal Analyses and Biological Properties of Novel F-Block Coordination Polymers Containing 2,2'-Thiodiacetic Acid and Piperazine. *Inorg. Chim. Acta* **2016**, *443*, 186–197. [[CrossRef](#)]
63. Zhang, Y.-Z.; Li, J.-R.; Gao, S.; Kou, H.-Z.; Sun, H.-L.; Wang, Z.-M. Two-Dimensional Rare Earth Coordination Polymers Involving Different Coordination Modes of Thiodiglycolic Acid. *Inorg. Chem. Commun.* **2002**, *5*, 28–31. [[CrossRef](#)]
64. Gans, P. GLEE, a New Computer Program for Glass Electrode Calibration. *Talanta* **2000**, *51*, 33–37. [[CrossRef](#)] [[PubMed](#)]
65. Petit, L.D.; Powell, K.J. *Stability Constants Database, SC-Database for Windows 1997*; Academic Software: Lokeren, Belgium, 1997.
66. Klungness, G.D.; Byrne, R.H. Comparative Hydrolysis Behavior of the Rare Earths and Yttrium: The Influence of Temperature and Ionic Strength. *Polyhedron* **2000**, *19*, 99–107. [[CrossRef](#)]
67. Martínez, S.; Igoa, F.; Carrera, I.; Seoane, G.; Veiga, N.; De Camargo, A.S.S.; Kremer, C.; Torres, J. A Zn(II) Luminescent Complex with a Schiff Base Ligand: Solution, Computational and Solid State Studies. *J. Coord. Chem.* **2018**, *71*, 874–889. [[CrossRef](#)]
68. *CrysAlisPro*, Version 2021; Rigaku Oxford Diffraction: Oxford, UK, 2021.
69. Sheldrick, G.M. SHELXT—Integrated Space-Group and Crystal-Structure Determination. *Acta Crystallogr. Sect. A Found. Adv.* **2015**, *71*, 3–8. [[CrossRef](#)]
70. Sheldrick, G.M. Crystal Structure Refinement with SHELXL. *Acta Crystallogr. Sect. C Struct. Chem.* **2015**, *71*, 3–8. [[CrossRef](#)]
71. Spek, A.L. Structure Validation in Chemical Crystallography. *Acta Crystallogr. D Biol. Crystallogr.* **2009**, *65*, 148–155. [[CrossRef](#)]
72. Dolomanov, O.V.; Bourhis, L.J.; Gildea, R.J.; Howard, J.A.K.; Puschmann, H. OLEX2: A Complete Structure Solution, Refinement and Analysis Program. *J. Appl. Crystallogr.* **2009**, *42*, 339–341. [[CrossRef](#)]
73. Bessen, N.P.; Popov, I.A.; Heathman, C.R.; Grimes, T.S.; Zalupski, P.R.; Moreau, L.M.; Smith, K.F.; Booth, C.H.; Abergel, R.J.; Batista, E.R.; et al. Complexation of Lanthanides and Heavy Actinides with Aqueous Sulfur-Donating Ligands. *Inorg. Chem.* **2021**, *60*, 6125–6134. [[CrossRef](#)] [[PubMed](#)]
74. Thakur, P.; Pathak, P.N.; Gedris, T.; Choppin, G.R. Complexation of Eu(III), Am(III) and Cm(III) with Dicarboxylates: Thermodynamics and Structural Aspects of the Binary and Ternary Complexes. *J. Solut. Chem.* **2009**, *38*, 265–287. [[CrossRef](#)]

75. Torres, J.; Peluffo, F.; Domínguez, S.; Mederos, A.; Arrieta, J.M.; Castiglioni, J.; Lloret, F.; Kremer, C. 2,2'-Oxydiacetato-Bridged Complexes Containing Sm(III) and Bivalent Cations. Synthesis, Structure, Magnetic Properties and Chemical Speciation. *J. Mol. Struct.* **2006**, *825*, 60–69. [[CrossRef](#)]
76. Grenthe, I.; Tobiasson, I.; Theander, O.; Hatanaka, A.; Munch-Petersen, J. Thermodynamic Properties of Rare Earth Complexes. I. Stability Constants for the Rare Earth Diglycolate Complexes. *Acta Chem. Scand.* **1963**, *17*, 2101–2112. [[CrossRef](#)]
77. Grenthe, I.; Gårdhammar, G.; Søtofte, I.; Beronius, P.; Engebretsen, J.E.; Ehrenberg, L. Thermodynamic Properties of Rare Earth Complexes. X. Complex Formation in Aqueous Solution of Eu(III) and Iminodiacetic Acid. *Acta Chem. Scand.* **1971**, *25*, 1401–1407. [[CrossRef](#)]
78. Chung, D.Y.; Lee, E.H.; Kimura, T. Laser-Induced Luminescence Study of Samarium(III) Thiodiglycolate Complexes. *Bull. Korean Chem. Soc.* **2003**, *24*, 1396–1398.
79. Lis, S.; Choppin, G.R. Luminescence Study of Europium(III) Complexes with Several Dicarboxylic Acids in Aqueous Solution. *J. Alloys Compd.* **1995**, *225*, 257–260. [[CrossRef](#)]
80. Dellien, I.; Grenthe, I.; Hessler, G. Thermodynamic Properties of Rare Earth Complexes XVIII. Free Energy, Enthalpy and Entropy Changes for the Formation of Some Lanthanoid Thiodiacetate and Hydrogen Thiodiacetate Complexes. *Acta Chem. Scandinava* **1973**, *27*, 2431–2440. [[CrossRef](#)]
81. Puentes, R.; Torres, J.; Kremer, C.; Cano, J.; Lloret, F.; Capucci, D.; Bacchi, A. Mononuclear and Polynuclear Complexes Ligated by an Iminodiacetic Acid Derivative: Synthesis, Structure, Solution Studies and Magnetic Properties. *Dalton Trans.* **2016**, *45*, 5356–5373. [[CrossRef](#)]
82. Casanova, D.; Llunell, M.; Alemany, P.; Alvarez, S. The Rich Stereochemistry of Eight-Vertex Polyhedra: A Continuous Shape Measures Study. *Chem.-Eur. J.* **2005**, *11*, 1479–1494. [[CrossRef](#)]
83. Llunell, M.; Casanova, D.; Cirera, J.; Alemany, P.; Alvarez, S. *SHAPE*, Version 1.1; Universitat de Barcelona: Barcelona, Spain, 2003.
84. Bünzli, J.-C.G. On the Design of Highly Luminescent Lanthanide Complexes. *Coord. Chem. Rev.* **2015**, *293–294*, 19–47. [[CrossRef](#)]
85. Thomsen, M.S.; Nawrocki, P.R.; Kofod, N.; Sørensen, T.J. Seven Europium(III) Complexes in Solution—The Importance of Reporting Data When Investigating Luminescence Spectra and Electronic Structure. *Eur. J. Inorg. Chem.* **2022**, *2022*, e202200334. [[CrossRef](#)]
86. Binnemans, K. Interpretation of Europium(III) Spectra. *Coord. Chem. Rev.* **2015**, *295*, 1–45. [[CrossRef](#)]

**Disclaimer/Publisher's Note:** The statements, opinions and data contained in all publications are solely those of the individual author(s) and contributor(s) and not of MDPI and/or the editor(s). MDPI and/or the editor(s) disclaim responsibility for any injury to people or property resulting from any ideas, methods, instructions or products referred to in the content.